2014

Bulk properties of solution-synthesized chevron-like graphene nanoribbons

Timothy H. Vo
University of Nebraska – Lincoln

Mikhail Shekhirev
University of Nebraska – Lincoln

Alexey Lipatov
University of Nebraska-Lincoln, alipatov@unl.edu

Rafal A. Korlacki
University of Nebraska-Lincoln, rkorlacki2@unl.edu

Alexander Sinitskii
University of Nebraska – Lincoln, sinitskii@unl.edu

Faraday Discussions

Cite this: *Faraday Discuss.*, 2014, **173**, 105

PAPER

Bulk properties of solution-synthesized chevron-like graphene nanoribbons

Timothy H. Vo,[a] Mikhail Shekhirev,[a] Alexey Lipatov,[a] Rafal A. Korlacki[b] and Alexander Sinitskii*[ac]

Received 13th June 2014, Accepted 3rd July 2014
DOI: 10.1039/c4fd00131a

Graphene nanoribbons (GNRs) have received a great deal of attention due to their promise for electronic and optoelectronic applications. Several recent studies have focused on the synthesis of GNRs by the bottom-up approaches that could yield very narrow GNRs with atomically precise edges. One type of GNRs that has received a considerable attention is the chevron-like GNR with a very distinct periodic structure. Surface-assisted and solution-based synthetic approaches for the chevron-like GNRs have been developed, but their electronic properties have not been reported yet. In this work, we synthesized chevron-like GNRs in bulk by a solution-based method, characterized them by a number of spectroscopic techniques and measured their bulk conductivity. We demonstrate that solution-synthesized chevron-like GNRs are electrically conductive in bulk, which makes them a potentially promising material for applications in organic electronics and photovoltaics.

1 Introduction

Graphene nanoribbons (GNRs), few-nm-wide strips of graphene, possess interesting electronic and optical properties.[1–6] While GNRs have long been considered theoretically,[1,2] the active experimental research in this area started less than a decade ago. Several recent studies have focused on the synthesis of GNRs by the bottom-up approaches that rely on building GNRs from smaller molecular species.[7–20] The resulting GNRs are very narrow (typically with widths, $w < 2$ nm) and have atomically precise edges, which is very important for potential applications.[3–6,21,22] One type of synthetic GNRs that has received considerable theoretical[23–25] and experimental attention[9,16,19,20,26] is the chevron-like GNR that has a very distinct periodic structure (Fig. 1a). Chevron-like GNRs were first synthesized by Cai *et al.* by the surface-assisted approach that involved coupling molecular precursors into linear polyphenylenes on Au(111) single crystals followed by

[a]*Department of Chemistry, University of Nebraska – Lincoln, Lincoln, NE 68588, USA. E-mail: sinitskii@unl.edu*
[b]*Department of Electrical Engineering, University of Nebraska – Lincoln, Lincoln, NE 68588, USA*
[c]*Nebraska Center for Materials and Nanoscience, University of Nebraska – Lincoln, Lincoln, NE 68588, USA*

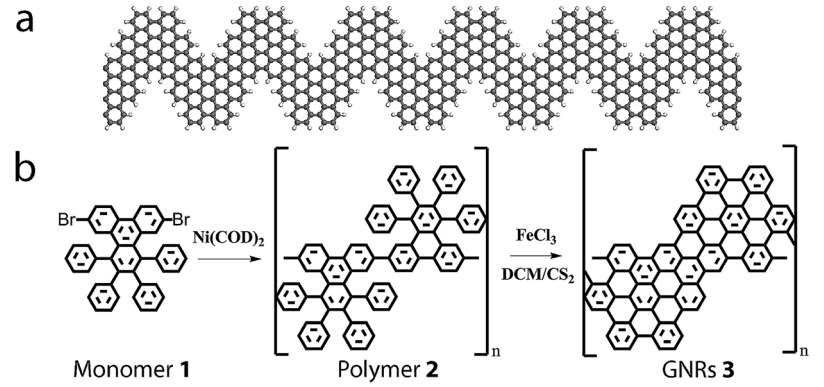

Fig. 1 Synthesis of chevron-like GNRs. (a) Schematic of a chevron-like GNR. (b) Scheme of the GNR synthesis; see text for details.

cyclodehydrogenation.[9] Later the solution-based synthetic approach for bulk quantities of chevron-like GNRs that relies on Yamamoto coupling of molecular precursors followed by cyclodehydrogenation *via* a Scholl reaction has also been demonstrated.[19,20]

Considering the potential use of GNRs in electronics[27–29] it is very important to understand their electronic properties. Despite some recent attempts to measure the electronic properties of GNRs synthesized by the bottom-up approaches[30,31] the electrical characterization of GNRs remains challenging in general and no conductivity measurements have been performed on chevron-like GNRs in particular. In this work, we synthesized chevron-like GNRs in bulk by a solution-based method,[19] confirmed their quality by scanning tunnelling microscopy (STM) and a number of spectroscopic techniques, and measured their bulk conductivity.

2 Experimental

All starting materials and solvents were purchased and used as received without any purification. Sodium hydroxide (97%), nitromethane (98%), iron(III) chloride (anhydrous, 98%), carbon disulphide and gold foil (0.025 mm, 99.985%) were purchased from Alfa Aesar. Methanol and mesitylene were purchased from Sigma-Aldrich. Acetone and dichloromethane were purchased from Fisher Scientific, and concentrated hydrochloric acid was purchased from Macron. Four-inch heavily p-doped silicon wafers with a 300 nm-thick layer of SiO_2 were purchased from Silicon Quest International.

Fig. 1b shows the scheme of the solution synthesis of chevron-like GNRs. We used the synthetic procedure that we disclosed in our previous work,[19] although with some modifications. We first synthesized the precursor monomer **1** and then converted it to the polymer **2** using bis(1,5-cyclooctadiene)nickel(0) ($Ni(COD)_2$) as described in our previous work.[19] We previously performed the cyclodehydrogenation of the polymer **2** with $FeCl_3$ to form GNRs using dichloromethane (DCM) as a solvent.[19] In the present work we preformed this reaction in a DCM–CS_2 mixture (1 : 1), since this mixture was shown to be an effective solvent

for cyclodehydrogenation of other polyphenylenes *via* the Scholl reaction.[32] More specifically, 50 mg of polymer **2** was added to 80 ml of DCM–CS_2 mixture (1 : 1) and sonicated until well-dispersed. The reaction mixture was degassed with nitrogen gas. Iron(III) chloride (1.666 g) was dissolved in nitromethane (5 ml) and added to the reaction mixture. The nitrogen gas was bubbled through the reaction mixture for 24 h. After that another portion of DCM–CS_2 (1 : 1) (60 ml) was added to the reaction mixture and the reaction was continued for another 7 h. The reaction mixture was then filtered and washed with concentrated hydrochloric acid, acetone, water, methanol, a methanol–sodium hydroxide mixture, methanol, water, and finally acetone. The resulting black solid was dried at 65 °C, yielding 49 mg of a black powder.

A Raman spectrum of GNRs deposited on Si/SiO_2 substrate was recorded using a Thermo Scientific DXR Raman microscope with a 532 nm laser.

UV-vis-NIR measurements of GNRs were performed using a Jasco V-670 spectrophotometer. GNR powder (2 mg) was added to 7 ml of mesitylene and sonicated at 80–90 °C for 90 s. The mixture was then refluxed for 10 min and sonicated at 80–90 °C for 30 s. The reflux and sonication steps were repeated one more time. Finally, the GNR dispersion in mesitylene was heated to reflux and transferred to a cuvette for UV-vis-NIR measurements while still hot.

X-ray photoelectron spectroscopy (XPS) was performed using a PHI Quantera SXM scanning X-ray microprobe. To prepare XPS samples several droplets of a GNR suspension in DCM were deposited on a gold foil and dried in air.

GNRs were deposited on a Au(111) substrate and imaged by scanning tunnelling microscopy (STM). To prepare a sample for STM measurements ~2 mg of GNRs powder was mixed with ~5 ml of mesitylene in a 100 ml round-bottom flask. The mixture was sonicated for 1 min and then heated to reflux while agitated for 5 min and then sonicated for another 30 s. The reflux-sonication procedure was repeated several times to the total of ~2.5 min of sonication time. Using a glass pipette, two drops of the GNR suspension in mesitylene were deposited while still hot ($T > 100$ °C) on the Au(111) substrate. The STM imaging was performed using a commercial Pt–Ir tip and a home-built ultrahigh vacuum (UHV) variable temperature STM system at the Center for Nanophase Materials Science (CNMS) at Oak Ridge National Laboratory (ORNL); the base pressure was lower than 1×10^{-10} mbar. The GNR samples were degassed in UHV for several hours before performing the STM measurements.

Fourier transform infrared (FTIR) spectroscopy of GNRs was preformed using a Nicolet Avatar 360 FTIR instrument. The measurements were performed on a small amount of a GNR powder that was placed directly on the spectrometer sample stage.

The electrical measurements of GNRs were performed using an Agilent 4155C Semiconductor Parameter Analyzer that was connected to a computer through 82357B USB/GPIB Interface and controlled using National Instruments LabView software. GNRs were measured in the form of pressed pellets (diameter, $d = 7$ mm, thickness, $t \sim 0.1$ mm) that were prepared using a hand press (International Crystal Laboratories). Prior to some of the electrical measurements the GNR pellets were annealed at 200 °C in a tube furnace (Lindberg/Blue M) in H_2/Ar (5 sccm of H_2, 5 sccm of Ar, total pressure ~500 mTorr) for 2 h.

Theoretical calculations were performed using a plane-wave density functional theory code Quantum ESPRESSO,[33] with the combination of the

exchange–correlation functional of Perdew, Burke, and Ernzerhof (PBE)[34] together with norm-conserving pseudopotentials developed by the Rappe Group.[35] The smallest repetition unit of the studied nanoribbon was placed in an orthorhombic cell, propagating along the *X*-direction and maintaining separation of at least 20 bohr (approx. 10.6 Å) on the vacuum sides (*Y* and *Z*). A large cutoff of 100 Ry for the electronic wavefunction and a tight convergence threshold of 1×10^{-12} for self-consistency were used throughout the calculations. The phonon frequencies and Raman activities were computed at the Γ point of the Brillouin zone using density-functional perturbation-theory for phonons[36] and second-order response for Raman activities,[37] for a structure previously relaxed to the level of reasonably small forces ($<6.0 \times 10^{-4}$ Ry per bohr).

3 Results and discussion

In order to confirm the high quality of GNRs that were prepared using the modified synthetic procedure, they were characterized by a number of analytical techniques. First of all, we used Raman spectroscopy, a technique known to be very sensitive to the disorder in carbon materials. Fig. 2a shows a comparison of theoretical and experimental Raman spectra of chevron-like GNRs. According to the results of the theoretical simulations, the Raman spectrum of chevron-like GNRs should exhibit not only the D and G bands (the most intense peaks in the spectrum around 1300 cm^{-1} and 1600 cm^{-1}, respectively) that are standard for graphene-based materials,[38] but also a series of smaller bands that are characteristic for this particular nanoribbon; these smaller bands are shown by arrows in the inset in Fig. 2a. These smaller bands include the fine structure of three peaks at the low-energy side of the G band, as well as the series of peaks around the D band. These features could be observed in the experimental spectrum of the chevron-like GNRs, which indicates their high structural quality.

We also used FTIR spectroscopy to confirm the efficiency of the oxidative cyclodehydrogenation of the polymer **2** to form GNRs **3** (see the last step in the reaction scheme shown in Fig. 1b) and the structural quality of the chevron-like GNRs. Fig. 2b demonstrates representative spectral regions for the material before and after cyclodehydrogenation, as well as the theoretical spectrum of the GNRs **3**. The left panel in Fig. 2b shows the spectral range from 3100 to 2850 cm^{-1} where the FTIR spectrum of the polymer **2** contains three characteristic peaks at 3077, 3053 and 3024 cm^{-1} that originate from the aromatic C–H stretching.[14,39] These peaks are not observed in the FTIR spectrum of GNRs **3**, which is in agreement with the theoretical spectrum, according to which the chevron-like GNRs should exhibit no peaks in this spectral range. Similar conclusions could be drawn from the analysis of the FTIR spectra of the polymer **2** and GNRs **3** in the spectral range from 900 to 650 cm^{-1}, see the right panel in Fig. 2b. The theoretical spectrum of the chevron-like GNRs is very different from the experimental FTIR spectrum of the polymer **2**, but, as expected, is in a good agreement with the experimental FTIR spectrum of GNRs **3**. In the polymer **2** spectrum the most intense peak at 697 cm^{-1}, which is typical for monosubstituted benzene rings,[14,39] nearly disappears after the oxidative cyclodehydrogenation of the polymer **2** to form GNRs **3** (Fig. 2b), and the remaining small peak actually matches well the similarly small peak in the theoretical spectrum of the chevron-like GNRs.

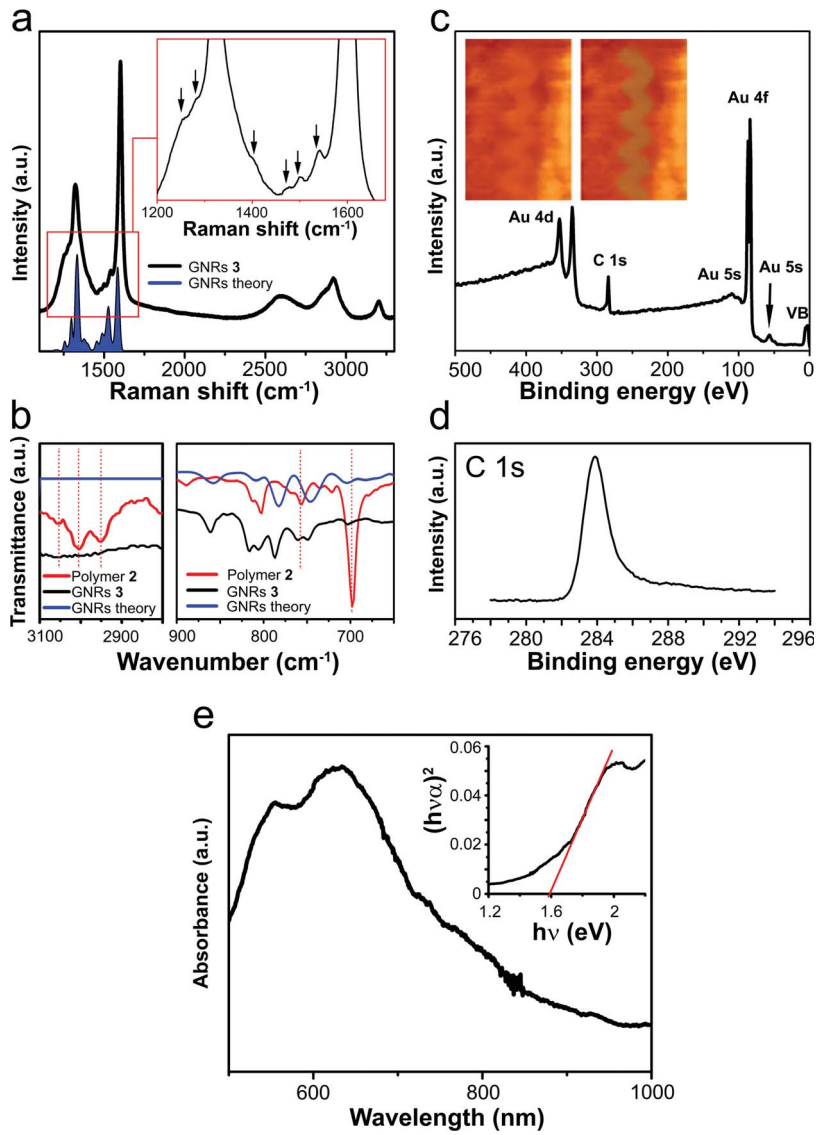

Fig. 2 Spectroscopic and microscopic characterization of GNRs. (a) Raman spectrum of GNRs. The black arrows in the inset show small peaks around D and G bands. (b) Comparison of the experimental FTIR spectra of the polymer **2**, GNRs **3**, and theoretical FTIR spectrum of GNRs **3**. (c and d) XPS spectra of GNRs deposited on a gold substrate: (c) survey spectrum, (d) C 1s spectrum. The inset in (c) shows 2.8 × 4.3 nm^2 STM image of a GNR deposited on Au(111) substrate; the left panel shows the original image, and the right panel shows the same image where the GNR is highlighted for the sake of clarity. (e) UV-vis-NIR absorbance spectrum of GNRs suspended in mesitylene. The inset shows the analysis of the energy-dependent absorbance of GNRs suspended in mesitylene, demonstrating an optical bandgap of ~1.6 eV.

Overall, the FTIR spectroscopy results confirm the efficient transformation of the polymer **2** to GNRs **3** (Fig. 1b), and the structural quality of the resulting nanoribbons.

To further demonstrate the high quality of these GNRs we visualized them by STM. The inset in Fig. 2c shows STM image of a GNR that was deposited on Au(111) substrate; the left panel shows the original image, while in the right panel the GNR is highlighted in green for the sake of clarity. The structure of the GNR observed in this STM image is in perfect agreement with the atomic structure shown in Fig. 1a.

The chemical purity of the GNRs was confirmed using XPS spectroscopy. Fig. 2c shows the XPS survey spectrum of GNRs deposited on a gold substrate. No peaks other than the C 1s peak and the peaks associated with the gold substrate could be observed in this spectrum, suggesting that possible impurities could be present in the sample only in amounts below the XPS detection limit. Fig. 2d shows the XPS C 1s spectrum of GNRs, demonstrating only a single sharp component at 284.5 eV corresponding to the sp^2 carbon atoms, as expected for a graphene-based material.

Fig. 2e shows a UV-vis-NIR spectrum of the chevron-like GNRs dispersed in mesitylene. The GNRs have strong absorption in UV and visible regions, which then decreases toward the NIR region and becomes negligible at $\lambda \sim 950$ nm ($E \sim 1.3$ eV), The linearization of the energy-dependent absorbance of the GNRs (see the inset in Fig. 2e) gives an optical band gap of $\sim$1.6 eV, which is very close to the theoretical band gap value of 1.57 eV that was previously calculated using the density functional theory (DFT) method.[9,19]

The electrical measurements were performed on pressed GNR pellets using the home-built setup shown in Fig. 3a. A GNR pellet was placed between two aluminium electrodes surrounded by a dielectric cylinder ("inner shell"). The dielectric outer shell was gently pressed to the bottom electrode using two screws to ensure good contact between the electrodes and GNR pellet. The electrodes were connected to a parameter analyzer for electrical measurements. Fig. 3b shows a typical GNR pellet that is 7 mm in diameter and has a thickness of $\sim$0.1 mm. Interestingly, although the GNR pellet has a black colour (Fig. 3b, left panel), it also has a characteristic metallic luster (Fig. 3b, right panel), thus somewhat resembling a graphite flake.

Two-terminal voltage–current (I–V) curves were measured in the voltage range from -5 to +5 V. Fig. 3c shows that the as-prepared GNR pellet is fairly conductive, showing a current of the order of a few microamperes in the given voltage range. The conductivity could be improved if the GNR pellet is annealed at 200 °C in H_2/Ar, as shown in Fig. 3c. The fact that the chevron-like GNRs are electrically conductive is an important result, considering the promise of bottom-up synthesized GNRs for organic electronics.[40,41]

It should also be noted that Fig. 3c illustrates the bulk conductivity of ribbons rather than represents the intrinsic electronic properties of an individual chevron-like GNR. An appropriate analogy can be made with carbon nanotubes (CNTs) that, similarly to GNRs, are also one-dimensional graphene-based materials. It is well-known that while CNTs have remarkable electronic properties, the electrical conductivities of CNTs fibers and composites are much lower than those of individual CNTs by at least one order of magnitude even for the rigorously optimized samples.[42] The electrical conductivity of a macroscopic CNT sample is affected by various structural imperfections that include poor intertube junctions, insufficient packing density, poor alignment of the CNTs, *etc.* In analogy with CNT fibers and composites, a bulk GNR sample (Fig. 3b) should have similar

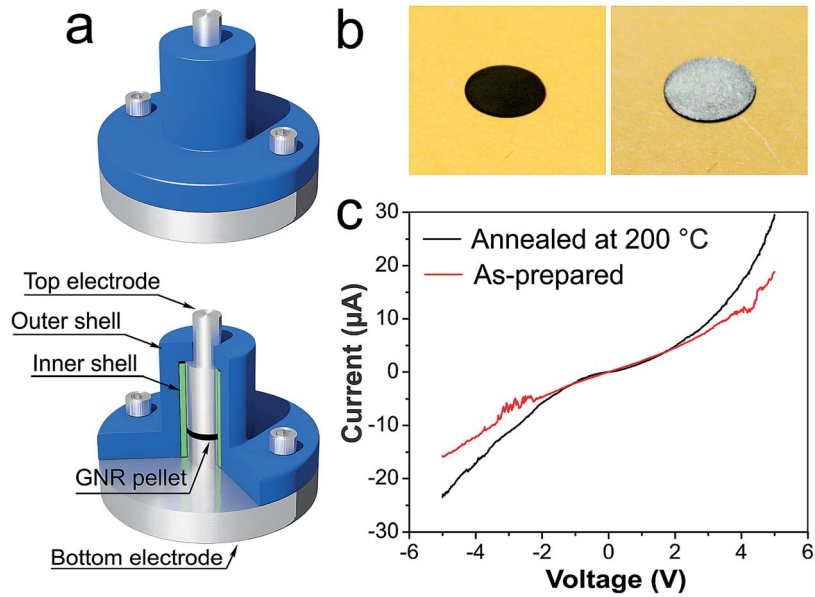

Fig. 3 Electrical measurements of GNRs. (a) Scheme of experimental setup for electrical measurements of GNRs. Top and bottom panels show the side view and the cross-section view of the setup, respectively. (b) Optical photographs of the as-prepared GNR pellet at different angles of observation. (c) Current–voltage (I–V) plots for the as-prepared and annealed GNR pellets.

structural imperfections, such as inefficient ribbon-to-ribbon junctions, low packing density of GNRs, and their poor alignment. Therefore, electrical measurements of individual chevron-like GNRs, as well as additional studies of different arrangements of GNRs, such as thin films and fibers, will be important to reveal the potential of this material for future applications.

4 Conclusions

In summary, we synthesized chevron-like GNRs in bulk by a solution-based method, visualized them by STM and characterized them by a number of spectroscopic techniques. We demonstrate that the as-synthesized chevron-like GNRs are electrically conductive in bulk, and the bulk conductivity of GNRs could be further improved by annealing in H_2/Ar. Electrical measurements of individual nanoribbons are still in order to better understand their electronic properties. However, the fact that the chevron-like GNRs are electrically conductive makes them a promising object for the future studies of the bulk applications of bottom-up synthesized GNRs in areas, such as GNR-based electronics and photovoltaics.

Acknowledgements

This work was supported by the Nebraska Center for Energy Sciences Research (#12-00-13), the Nebraska Research Initiative and the NSF through Nebraska MRSEC (DMR-0820521) and EPSCoR (EPS-1004094). STM imaging of GNRs was

performed in the framework of the CNMS ORNL user project (CNMS2013-349); we thank Jun Wang and Minghu Pan for STM assistance. This research was performed in part in the Central Facilities of the Nebraska Center for Materials and Nanoscience, which is supported by the Nebraska Research Initiative. Theoretical calculations were performed using the resources of the Holland Computing Center at the University of Nebraska-Lincoln.

References

1 M. Fujita, K. Wakabayashi, K. Nakada and K. Kusakabe, *J. Phys. Soc. Jpn.*, 1996, **65**, 1920.
2 K. Nakada, M. Fujita, G. Dresselhaus and M. S. Dresselhaus, *Phys. Rev. B: Condens. Matter Mater. Phys.*, 1996, **54**, 17954.
3 V. Barone, O. Hod and G. E. Scuseria, *Nano Lett.*, 2006, **6**, 2748.
4 L. Yang, C.-H. Park, Y.-W. Son, M. L. Cohen and S. G. Louie, *Phys. Rev. Lett.*, 2007, **99**, 186801.
5 L. Yang, M. L. Cohen and S. G. Louie, *Nano Lett.*, 2007, **7**, 3112.
6 D. Prezzi, D. Varsano, A. Ruini, A. Marini and E. Molinari, *Phys. Rev. B: Condens. Matter Mater. Phys.*, 2008, **77**, 041404.
7 X. Y. Yang, X. Dou, A. Rouhanipour, L. J. Zhi, H. J. Rader and K. Mullen, *J. Am. Chem. Soc.*, 2008, **130**, 4216.
8 Y. Fogel, L. Zhi, A. Rouhanipour, D. Andrienko, H. J. Räder and K. Müllen, *Macromolecules*, 2009, **42**, 6878.
9 J. M. Cai, P. Ruffieux, R. Jaafar, M. Bieri, T. Braun, S. Blankenburg, M. Muoth, A. P. Seitsonen, M. Saleh, X. L. Feng, K. Mullen and R. Fasel, *Nature*, 2010, **466**, 470.
10 L. Dossel, L. Gherghel, X. L. Feng and K. Mullen, *Angew. Chem., Int. Ed.*, 2011, **50**, 2540.
11 A. Chuvilin, E. Bichoutskaia, M. C. Gimenez-Lopez, T. W. Chamberlain, G. A. Rance, N. Kuganathan, J. Biskupek, U. Kaiser and A. N. Khlobystov, *Nat. Mater.*, 2011, **10**, 687.
12 T. W. Chamberlain, J. Biskupek, G. A. Rance, A. Chuvilin, T. J. Alexander, E. Bichoutskaia, U. Kaiser and A. N. Khlobystov, *ACS Nano*, 2012, **6**, 3943.
13 S. Blankenburg, J. M. Cai, P. Ruffieux, R. Jaafar, D. Passerone, X. L. Feng, K. Mullen, R. Fasel and C. A. Pignedoli, *ACS Nano*, 2012, **6**, 2020.
14 M. G. Schwab, A. Narita, Y. Hernandez, T. Balandina, K. S. Mali, S. De Feyter, X. L. Feng and K. Mullen, *J. Am. Chem. Soc.*, 2012, **134**, 18169.
15 Y.-C. Chen, D. G. de Oteyza, Z. Pedramrazi, C. Chen, F. R. Fischer and M. F. Crommie, *ACS Nano*, 2013, **7**, 6123.
16 C. Bronner, S. Stremlau, M. Gille, F. Braußе, A. Haase, S. Hecht and P. Tegeder, *Angew. Chem., Int. Ed.*, 2013, **52**, 4422.
17 K. T. Kim, J. W. Lee and W. H. Jo, *Macromol. Chem. Phys.*, 2013, **214**, 2768.
18 A. Narita, X. Feng, Y. Hernandez, S. A. Jensen, M. Bonn, H. Yang, I. A. Verzhbitskiy, C. Casiraghi, M. R. Hansen, A. H. R. Koch, G. Fytas, O. Ivasenko, B. Li, K. S. Mali, T. Balandina, S. Mahesh, S. De Feyter and K. Mullen, *Nat. Chem.*, 2014, **6**, 126.
19 T. H. Vo, M. Shekhirev, D. A. Kunkel, M. D. Morton, E. Berglund, L. M. Kong, P. M. Wilson, P. A. Dowben, A. Enders and A. Sinitskii, *Nat. Commun.*, 2014, **5**, 3189.

20 T. H. Vo, M. Shekhirev, D. A. Kunkel, F. Orange, M. J. F. Guinel, A. Enders and A. Sinitskii, *Chem. Commun.*, 2014, **50**, 4172.
21 D. A. Areshkin, D. Gunlycke and C. T. White, *Nano Lett.*, 2006, **7**, 204.
22 E. R. Mucciolo, A. H. Castro Neto and C. H. Lewenkopf, *Phys. Rev. B: Condens. Matter Mater. Phys.*, 2009, **79**, 075407.
23 E. Costa Girão, L. Liang, E. Cruz-Silva, A. G. S. Filho and V. Meunier, *Phys. Rev. Lett.*, 2011, **107**, 135501.
24 S. D. Wang and J. L. Wang, *J. Phys. Chem. C*, 2012, **116**, 10193.
25 L. Liang and V. Meunier, *Phys. Rev. B: Condens. Matter Mater. Phys.*, 2012, **86**, 195404.
26 S. Linden, D. Zhong, A. Timmer, N. Aghdassi, J. H. Franke, H. Zhang, X. Feng, K. Müllen, H. Fuchs, L. Chi and H. Zacharias, *Phys. Rev. Lett.*, 2012, **108**, 216801.
27 X. R. Wang, Y. J. Ouyang, X. L. Li, H. L. Wang, J. Guo and H. J. Dai, *Phys. Rev. Lett.*, 2008, **100**, 206803.
28 A. Sinitskii, A. Dimiev, D. V. Kosynkin and J. M. Tour, *ACS Nano*, 2010, **4**, 5405.
29 J. Baringhaus, M. Ruan, F. Edler, A. Tejeda, M. Sicot, A. Taleb-Ibrahimi, A. P. Li, Z. G. Jiang, E. H. Conrad, C. Berger, C. Tegenkamp and W. A. de Heer, *Nature*, 2014, **506**, 349.
30 P. B. Bennett, Z. Pedramrazi, A. Madani, Y.-C. Chen, D. G. de Oteyza, C. Chen, F. R. Fischer, M. F. Crommie and J. Bokor, *Appl. Phys. Lett.*, 2013, **103**, 253114.
31 A. N. Abbas, G. Liu, A. Narita, M. Orosco, X. Feng, K. Müllen and C. Zhou, *J. Am. Chem. Soc.*, 2014, **136**, 7555.
32 C. D. Simpson, G. Mattersteig, K. Martin, L. Gherghel, R. E. Bauer, H. J. Rader and K. Mullen, *J. Am. Chem. Soc.*, 2004, **126**, 3139.
33 P. Giannozzi, S. Baroni, N. Bonini, M. Calandra, R. Car, C. Cavazzoni, D. Ceresoli, G. L. Chiarotti, M. Cococcioni, I. Dabo, A. Dal Corso, S. de Gironcoli, S. Fabris, G. Fratesi, R. Gebauer, U. Gerstmann, C. Gougoussis, A. Kokalj, M. Lazzeri, L. Martin-Samos, N. Marzari, F. Mauri, R. Mazzarello, S. Paolini, A. Pasquarello, L. Paulatto, C. Sbraccia, S. Scandolo, G. Sclauzero, A. P. Seitsonen, A. Smogunov, P. Umari and R. M. Wentzcovitch, *J. Phys. Condens. Matter.*, 2009, **21**, 395502.
34 J. P. Perdew, K. Burke and M. Ernzerhof, *Phys. Rev. Lett.*, 1996, **77**, 3865.
35 http://www.sas.upenn.edu/rappegroup/research/pseudo-potential-gga.html.
36 S. Baroni, S. de Gironcoli, A. Dal Corso and P. Giannozzi, *Rev. Mod. Phys.*, 2001, **73**, 515.
37 M. Lazzeri and F. Mauri, *Phys. Rev. Lett.*, 2003, **90**, 036401.
38 A. C. Ferrari and D. M. Basko, *Nat. Nanotechnol.*, 2013, **8**, 235.
39 A. Centrone, L. Brambilla, T. Renouard, L. Gherghel, C. Mathis, K. Müllen and G. Zerbi, *Carbon*, 2005, **43**, 1593.
40 S. A. Jensen, R. Ulbricht, A. Narita, X. Feng, K. Müllen, T. Hertel, D. Turchinovich and M. Bonn, *Nano Lett.*, 2013, **13**, 5925.
41 M. El Gemayel, A. Narita, L. F. Dossel, R. S. Sundaram, A. Kiersnowski, W. Pisula, M. R. Hansen, A. C. Ferrari, E. Orgiu, X. Feng, K. Mullen and P. Samori, *Nanoscale*, 2014, **6**, 6301.
42 N. Behabtu, C. C. Young, D. E. Tsentalovich, O. Kleinerman, X. Wang, A. W. K. Ma, E. A. Bengio, R. F. ter Waarbeek, J. J. de Jong, R. E. Hoogerwerf, S. B. Fairchild, J. B. Ferguson, B. Maruyama, J. Kono, Y. Talmon, Y. Cohen, M. J. Otto and M. Pasquali, *Science*, 2013, **339**, 182.